Journal of The Electrochemical Society

The Electrochemical Society
Advancing solid state & electrochemical science & technology

Solubility, Activity Coefficients and the Separation Factor of U/Pr Couple in Ga-In Alloys of Different Compositions in Fused LiCl-KCl-CsCl Eutectic

To cite this article: Alena Novoselova and Valeri Smolenski 2020 *J. Electrochem. Soc.* **167** 126518

View the article online for updates and enhancements.

This content was downloaded from IP address 212.193.94.28 on 10/08/2021 at 12:45

Journal of The Electrochemical Society, 2020 **167** 126518
1945-7111/2020/167(12)/126518/9/$40.00 © 2020 The Electrochemical Society ("ECS"). Published on behalf of ECS by IOP Publishing Limited

Solubility, Activity Coefficients and the Separation Factor of U/Pr Couple in Ga-In Alloys of Different Compositions in Fused LiCl-KCl-CsCl Eutectic

Alena Novoselova[1,2,z] **and Valeri Smolenski**[1,2]

[1]*Institute of High-Temperature Electrochemistry UB RAS, Ekaterinburg 620990, Russia*
[2]*Department of Rare Metals and Nanomaterials, Institute of Physics and Technology, Ural Federal University, Ekaterinburg 620002, Russia*

The equilibrium potentials of Pr^{3+}/Pr couple, triple Pr–Ga–In and U-Ga-In alloys vs Cl^-/Cl_2 reference electrode at the temperature range 723–1073 K in fused LiCl-KCl-CsCl eutectic were carried out by open-circuit potentiometry. The principle thermodynamic properties, solubility and the activity coefficients of praseodymium in gallium-indium alloys, containing 20, 40 and 70 wt% indium were determined. It was established a strong interaction between atoms of Pr and liquid alloys. The temperature dependences of the separation factor of U/Pr couple vs the composition of gallium-indium alloys were calculated.
© 2020 The Electrochemical Society ("ECS"). Published on behalf of ECS by IOP Publishing Limited. [DOI: 10.1149/1945-7111/abb3d9]

Manuscript submitted June 3, 2020; revised manuscript received August 19, 2020. Published September 7, 2020.

The future of nuclear power is associated with fast neutron reactors, which can significantly increase fuel burn out and expand the reproduction of fissile materials. Dry regeneration technologies, including electrochemical methods, using thermally and radiation-resistant molten salts and metals, are being developed for accelerated processing of high-radiated low-energy fuel of fast neutron reactors. The liquid state of metal and salt at relatively low temperatures makes it easier to solve the important problem of the phase separation for radiochemical technology. It is particularly appropriate to use these methods for regulating the composition and continuous fuel regeneration of molten salts homogeneous reactors (MSR)—ready media for electrochemical processes. The possibilities and the ways to improve the electrochemical regeneration of spent nuclear fuel (SNF) can be revealed only on the basis of the development of the theory and experimental study of the joint electrode reactions in the molten salt—liquid metal system.[1–6]

Lanthanides (Ln) are one of the most dangerous fission products (FP), and therefore much attention has recently been paid to the study of their electrochemical properties in molten salts. The electrochemical behavior of lanthanides was investigated at different working electrodes in fused LiCl–KCl eutectic: (i) inert solid electrodes—tungsten, molybdenum; (ii) active liquid electrodes—Ga, Cd, Bi, Zn etc. It is known that lanthanides are electrochemically deposited on inert electrodes at potentials −3.1–3.2 V, and on liquid active electrodes with a depolarization of 0.4–0.5 V vs the chlorine reference electrode. In fact, different liquid electrodes such as Cd,[7–16] Bi,[7,8,17–20] Zn,[21–23] Al,[24–26] and Ga[27,28] were investigated for separation of actinides from lanthanides and also many research efforts were made toward to liquid Cd.

From the point of the efficiency of separating actinides from lanthanides, the following row of the low-melting active metals was proposed: Ga > Sn > Bi > In > Zn > Cd.[29] Analyzing this dependence one can see that gallium is the best as a prospective liquid metal but it is a trace element, and therefore is rather expensive for the industrial application. So, alloys of gallium with other elements, e.g. indium, can be employed instead of pure Ga. For this reason, a light-melting Ga-In alloys may be selected as a liquid metal solvent for selectively extracting of uranium and Plutonium from spent nuclear fuel with their almost complete return to the nuclear fuel cycle. It is known that Ga–In alloys are very prospective for reprocessing SNF.[30–36]

Praseodymium is one of the fission products and a neutron poison, so its separation from the base fuel components during reprocessing is mandatory. It is known that the chemical and electrochemical properties of lanthanides are close. It is difficult to judge their behavior in different systems *a priori*. Conclusions can be drawn only after conducting experiments.

The electrochemical behavior of oxygen free uranium compounds was studied in fused 3LiCl-2KCl eutectic by transient electrochemical methods on inert electrodes.[37–42] Also, the electrochemical behavior of uranium (III) ions on liquid gallium electrodes in fused 3LiCl-2KCl eutectic was investigated.[43] It was established that the electrode reaction was occurred in one step with the transfer of three electrons with the formation of intermetallic compound UGa_3. The activity coefficient and solubility of U in liquid Ga was determined. The Gibbs free energy change for the formation of UGa_3 compound was calculated.

The purpose of this research was the experimental determination the activity coefficients and solubility of praseodymium in Ga-base alloys, calculation of the principal thermodynamic properties of triple Pr–Ga–In alloys and the separation factor (SF) of Pr/U couple in the wide temperature range.

Experimental

Anhydrous lithium chloride (Aldrich-Sigma 99.99%), potassium chloride (OSC 5–4 Russia 99.9%), cesium chloride (OSC 5–4 Russia 99.94%), praseodymium trichloride (Aldrich-Sigma 99.99%), gallium metal (JSC "Pikalevo alumina plant," Russia 99.9999%) and indium metal (JSC "Pikalevo alumina plant," Russia 99.9995%) were used in experiments. Salts and metal mixtures of the required compositions were prepared from the individual components in glove box SPEKS GB02 (<1 ppm oxygen and <1 ppm moisture content). The exact composition of the triple eutectic was 57.5 mol% LiCl-16.5 mol% KCl-26.0 mol% CsCl.[44]

A standard three-electrode electrochemical cell was used for measuring the equilibrium potentials of the Pr^{3+}/Pr couple, triple Pr–Ga–In and U-Ga-In alloys. The working electrode (WE) was a molybdenum wire or a bimetallic alloy of a given composition. A glass-carbon rod was used as a counter electrode (CE). Measurements were carried out vs the Cl^-/Cl_2 reference electrode (RE)[34] at the temperature range 723–1073 K under dry argon atmosphere. The investigations were performed employing an AUTOLAB 302 N potentiostat-galvanostat station controlled by NOVA 1.11 software. The composition of Ga-In alloys was 20, 40 and 70 wt% and the amount of them was about 2–4 g placed in a berlox crucible. The salt mixture (70–90 g) for experiments was placed in the cell in a vitreous carbon crucible. Praseodymium containing alloys (dilute or saturated solutions) were prepared by electrolysis of LiCl-KCl-$PrCl_3$ melt directly in the experimental cell before the experiments. Preparation of dilute and saturated solutions of triple alloys was performed in the galvanostatic mode. The concentration of praseodymium (uranium) in dilute alloys did not

[z]E-mail: alena_novoselova@list.ru

exceed 0.5 wt%. Electrolysis current was equal to 5–10 mA, the duration of electrolysis was 50–70 min. For the obtaining of saturated solutions (liquid+intermetallic compound) the electrolysis current was 15–25 mA, and the duration exceeded 100 min. The uranium ions were introduced into electrolyte by anodic dissolution of metallic uranium. Uranium containing alloys were prepared by electrolysis of LiCl-KCl-UCl_3 melt. The following galvanic cells were used for measuring the equilibrium electrode potentials of Pr^{3+}/Pr, couples (1) and for the equilibrium electrode potentials of the alloys (2, 3) by open-circuit potentiometry (OCP):

$$(-)\mathrm{Mo(Pr)_{(s)}|LiCl-KCl-CsCl_{(eut.)}},\ \mathrm{Pr^{3+}{}_{(l)}} \\ \|\mathrm{LiCl-KCl-CsCl_{(eut.)}|C_{(s)},Cl_{2(g)}}\,(+) \qquad [1]$$

$$(-)\mathrm{Me(Ga-In)_{(dilute\ sol.)}|LiCl-KCl-CsCl_{(eut.)}Me^{3+}{}_{(l)}}, \\ \|\mathrm{LiCl-KCl-CsCl_{(eut.)}|C_{(s)},Cl_{2(g)}}(+) \qquad [2]$$

$$(-)\mathrm{Me(Ga-In)_{(satur.\ sol.)}|LiCl-KCl-CsCl_{(eut.)}},\quad \mathrm{Me^{3+}{}_{(l)}} \\ \|\mathrm{LiCl-KCl-CsCl_{(eut.)}|C_{(s)},Cl_{2(g)}}(+) \qquad [3]$$

After the experiments, a small amount of the alloy and a sample of solid salts were dissolved, respectively, in acid and in aqueous solutions. Method of high-temperature filtration of saturated Pr-Ga-In alloys through a porous quartz filter was used for the separation of liquid metallic alloys from solid intermetallic compounds. The concentration of praseodymium (uranium) in the samples was determined by the ICP-MS test.

Results and Discussion

The equilibrium electrode potential of the Pr^{3+}/Pr couple was measured by OCP method using galvanic cell (1). The inert molybdenum cathode was polarized with a current of 100–150 mA for 15–30 s, and then the potential—time dependence was recorded, Fig. 1. The obtained chronopotentiograms clearly show a plateau that correspond to the quasi-equilibrium potential Pr^{3+}/Pr couple. The value of the apparent standard electrode potential of $E^*_{Pr(III)/Pr}$ was calculated by Nernst Eq. 4[30–36]:

$$E_{Pr(III)/Pr} = E^*_{Pr(III)/Pr} + \frac{RT}{nF}\ln C_{Pr(III)}, \qquad [4]$$

where $E_{Pr(III)/Pr}$ is the equilibrium standard potential of the Pr^{3+}/Pr couple, V; $E^*_{Pr(III)/Pr}$ is the apparent standard potential of the Pr^{3+}/Pr couple, V; $C_{Pr(III)}$ is the concentration of the praseodymium ions in the solvent in mole fraction; R, T, n, F are standard values.

Variation of the apparent standard potentials of the couples Pr^{3+}/Pr as a function of the temperature is presented in Fig. 2 and described by the Eq. 4:

$$E^*_{Pr(III)/Pr} = -(3.759 \pm 0.016) + (8.6 \pm 0.2)\cdot 10^{-4}\cdot T \pm 0.011 \quad V \qquad [5]$$

The potential-time dependences of Pr-Ga-In alloy vs Cl^-/Cl_2 reference electrode after electrodeposition of praseodymium (III) ions on liquid (Ga-20 wt% In) electrode in LiCl-KCl-CsCl-$PrCl_3$ melt as a function of the polarization current at 891 K at inert atmosphere were presented in Fig. 3. At the polarization current of 5 mA, Fig. 3(1), no visible changes in the cathode surface were found, and after a short time, the cathode potential returned to its initial value. When the value of polarization current was 30 mA only the reaction of the intermetallic compound formation was recorded, Fig. 3(2). The quasi-equilibrium potential of electrode after polarization was in the range from −2.46 V till −2.41 V. A further increase of the current (80 mA) led to the formation of the intermetallic compounds of different composition, as it is shown in Fig. 3(3).

The potential-time dependences of U-Ga-In alloy vs Cl^-/Cl_2 reference electrode after electrodeposition of uranium on liquid (Ga-20 wt% In) electrode in the LiCl-KCl-CsCl-UCl_3 melt as a function of the polarization current at 876 K were presented in Fig. 4. At the polarization current of 1 mA, Fig. 4(1), no visible changes in the cathode surface were found, and after a short time, the cathode potential returned to its initial value. When the value of polarization current was 20 mA only the reaction of the intermetallic compound formation was recorded, Fig. 4(2). A further increase of the current up to 100 mA led to the formation of two-phase deposit. It was established the formation of intermetallic compounds of different composition at −2.2 V. Also, on the surface of liquid alloy electrode uranium metal dendrites was appeared at potential −2.6 V, Fig. 4(3).

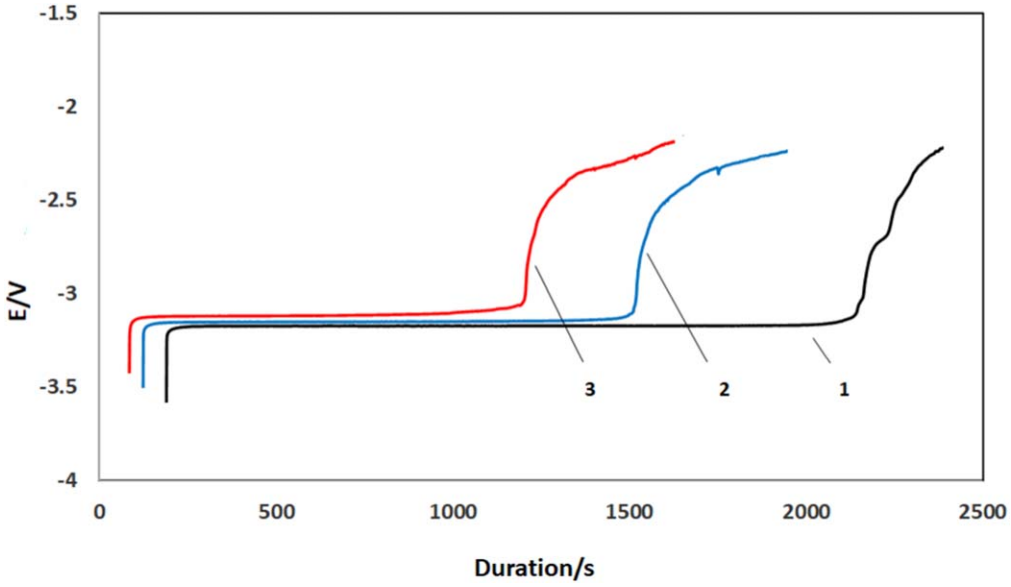

Figure 1. Chronopotentiograms of the LiCl-KCl-CsCl-$PrCl_3$ (2.93 wt%) melt vs the temperature on solid inert Mo electrode at inert atmosphere. Temperature: 1–751 K; 2–938 K; 3–1067 K.

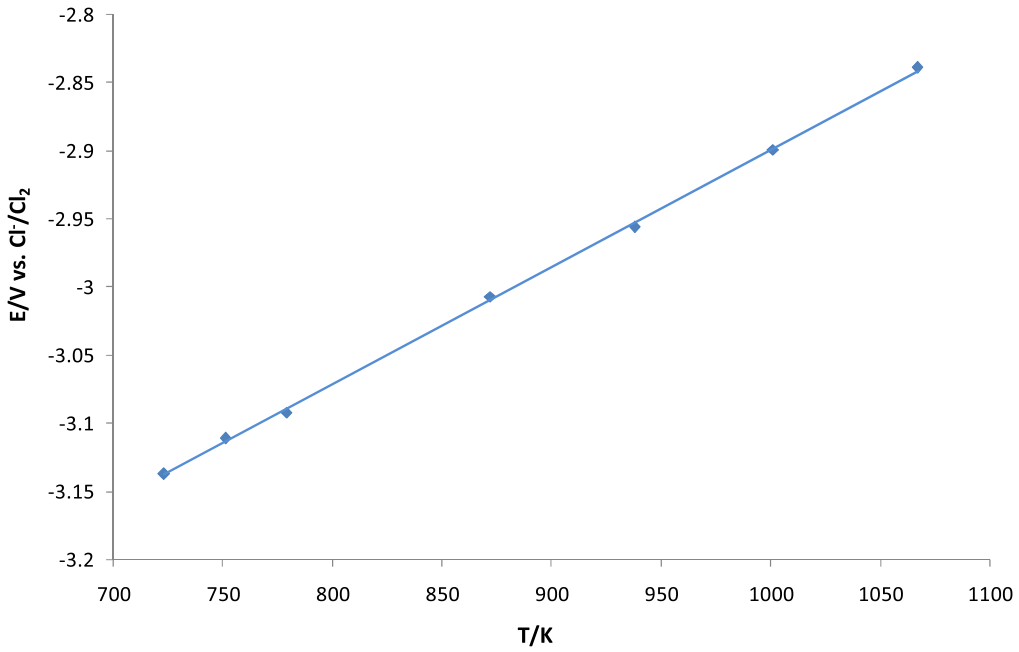

Figure 2. Variation of the apparent standard potential of $E^{*}_{Pr(III)/Pr}$ vs Cl^{-}/Cl_2 as a function of the temperature in fused LiCl-KCl-CsCl-$PrCl_3$ melt. Concentration of $PrCl_3$ in solvent—2.93 wt%.

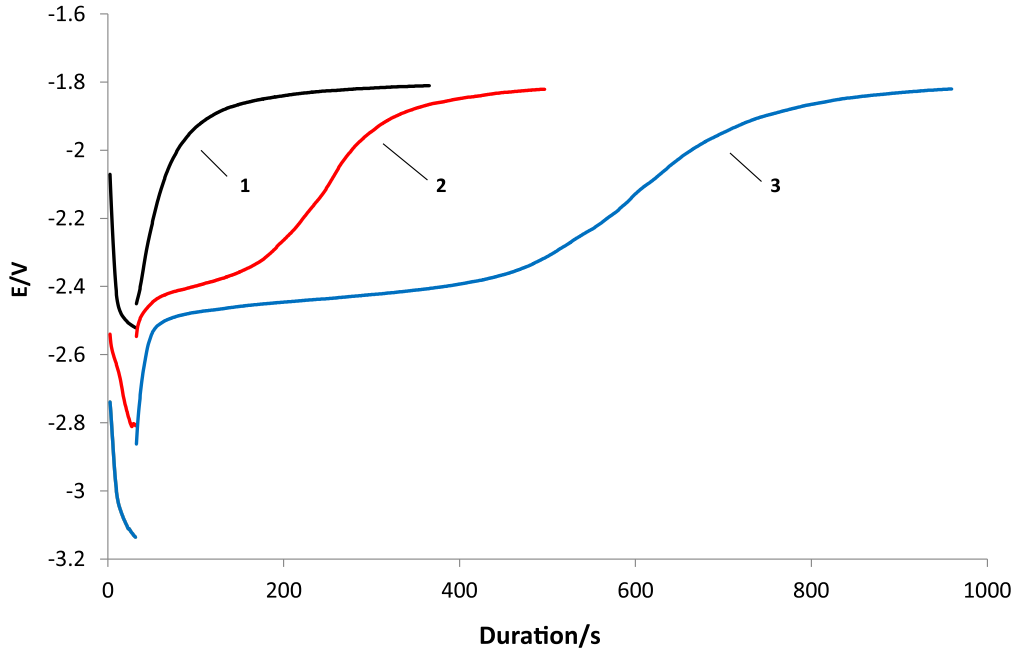

Figure 3. Chronopotentiograms of the LiCl-KCl-CsCl-$PrCl_3$ (2.02 wt%) melt vs polarization current on the liquid (Ga −20 wt% In) electrode at 891 K at inert atmosphere. Polarization current, mA: 1–5; 2–30; 3–80. Polarization time: 20–30 s. The surface of the electrode was equal to 0.47 cm^2. 1—No deposits on the liquid cathode; 2—Formation of the intermetallic compound; 3—Formation of the intermetallic compounds of different composition.

The obtained data in Figs. 3 and 4 allowed us to find the optimal conditions for obtaining dilute and saturated triple alloys compositions for further investigations.

For the dilute solutions of Me in liquid Ga-In alloys, the activity coefficient of the metal is constant. Therefore, the apparent standard potential $E^{**}_{Me(Ga-In)}$ of the alloy was described by the following expression[29]:

$$E_{Me(Ga-In)} = E^{**}_{Me(Ga-In)} + \frac{RT}{nF} \ln \frac{C_{Me(III)}}{x_{Me(Ga-In)}}, \qquad [6]$$

where Me = Pr or U; $E_{Me(Ga-In)}$ is equal the equilibrium potential of the alloy, V; $E^{**}_{Me(Ga-In)}$ is equal an apparent standard potential of the alloy, V; n is equal the number of exchanged electrons; $C_{Me(III)}$ is equal the concentration of the metal ions in solvent in mole fraction; $x_{Me(Ga-In)}$ is equal the concentration of the metal in the alloy in atomic fraction.

The calculated values of apparent standard potentials of Pr–Ga–In and U-Ga-In in fused LiCl-KCl-CsCl eutectic at different temperatures are presented in Tables I, II and Fig. 5. The experimental data was fitted by using the software Origin Pro 7.5 software:

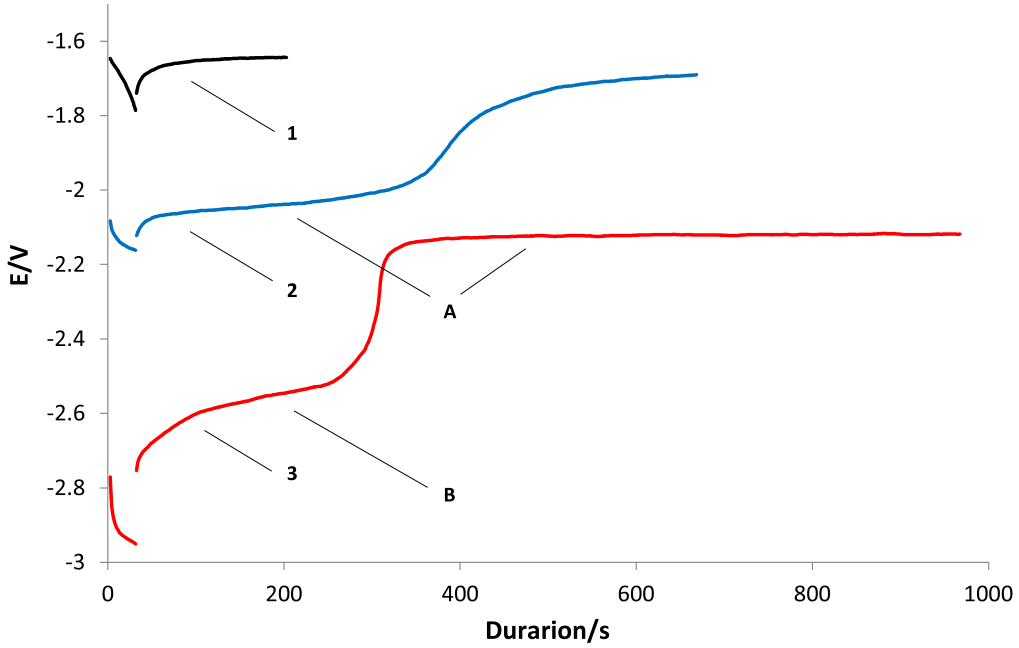

Figure 4. Chronopotentiograms of the LiCl-KCl-CsCl-UCl_3 (2.47 wt%) melt vs polarization current on the liquid (Ga −20 wt% In) electrode at 876 K at inert atmosphere. Polarization current, mA: 1–1; 2–20; 3–80. Polarization time: 15–30 s. The surface of the electrode was equal to 0.52 cm^2. 1—No deposits on the liquid cathode; 2—Formation of the intermetallic compound; 3—Formation of the intermetallic compounds of different composition and the uranium dendrites on the cathode surface.

Table I. Apparent standard potentials of Pr^{3+}/Pr couple and triple Pr-Ga-In alloys in fused Pr(Ga-In)/LiCl-KCl-CsCl system at different temperatures.

T/K	$E^{*}_{Pr(III)/Pr}$/V E^{**}/V	$E^{**}_{Pr(Ga-20\ wt\%\ In)}$/V E^{**}/V	$E^{**}_{Pr(Ga-40\ wt\%\ In)}$/V E^{**}/V	$E^{**}_{Pr(Ga-70\ wt\%\ In)}$/V E^{**}/V
723	−3.137	−2.479	−2.515	−2.562
751	−3.111	−2.451	−2.496	−2.549
779	−3.092	−2.439	−2.483	−2.529
872	−3.007	−2.382	−2.426	−2.468
938	−3.956	−2.335	−2.388	−2.435
1001	−2.899	−2.296	−2.347	−2.396
1067	−2.839	−2.257	−2.304	−2.351

$$E^{**}_{Pr(Ga-20wt\%\ In)} = -(3.061 \pm 0.025) + (7.9 \pm 0.3) \cdot 10^{-4} \cdot T \pm 0.016\ V \quad [7]$$

$$E^{**}_{Pr(Ga-40wt\%\ In)} = -(2.956 \pm 0.009) + (6.1 \pm 0.1) \cdot 10^{-4} \cdot T \pm 0.008\ V \quad [8]$$

$$E^{**}_{Pr(Ga-70wt\%\ In)} = -(3.009 \pm 0.022) + (6.2 \pm 0.6) \cdot 10^{-4} \cdot T \pm 0.023\ V \quad [9]$$

$$E^{**}_{U(Ga-20wt\%\ In)} = -(2.508 \pm 0.006) + (3.8 \pm 0.1) \cdot 10^{-4} \cdot T \pm 0.003\ V \quad [10]$$

$$E^{**}_{U(Ga-40wt\%\ In)} = -(2.558 \pm 0.011) + (3.9 \pm 0.2) \cdot 10^{-4} \cdot T \pm 0.014\ V \quad [11]$$

$$E^{**}_{U(Ga-70wt\%\ In)} = -(2.589 \pm 0.010) + (3.6 \pm 0.4) \cdot 10^{-4} \cdot T \pm 0.018\ V \quad [12]$$

The activity coefficients of α-Pr in liquid Ga–In bimetallic alloys were determined from the following equation[29]:

$$\log\ \gamma_{Pr(Ga-In)} = \frac{3F}{2.303RT}(E^{*}_{Pr(III)/Pr} - E^{**}_{Pr(Ga-In)}) \quad [13]$$

The activity coefficients of α-Pr in liquid Ga–In bimetallic alloys vs the temperature were fitted to the expressions (13–15) and presented in Table III.

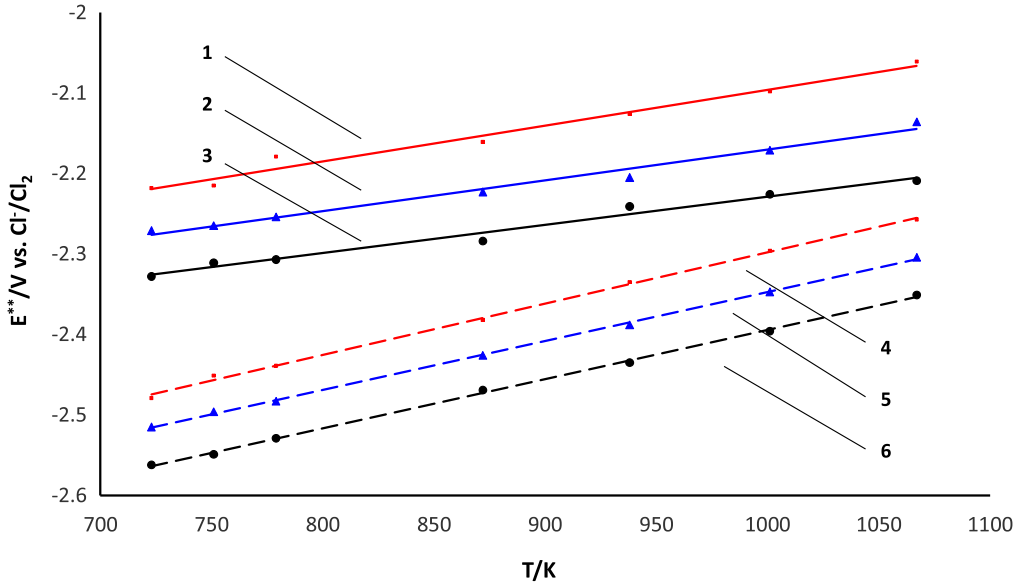

Figure 5. Variation of the apparent standard potentials of the alloy $E^{**}_{U(Ga-In)}$ and $E^{**}_{Pr(Ga-In)}$ vs Cl^-/Cl_2 as a function of the temperature in fused LiCl-KCl-CsCl eutectic. Concentration of Pr in alloy—0.69 wt%. Concentration of U in alloy—0.58 wt%. 1—U-Ga-20 wt% In; 2—U-Ga-40 wt% In; 3—U-Ga-70 wt% In.4—Pr-Ga-20 wt% In; 5—Pr-Ga-40 wt% In; 6—Pr-Ga-70 wt% In.

Table II. Apparent potentials of triple U-Ga-In alloys in fused U(Ga-In)/LiCl-KCl-CsCl system at different temperatures.

T/K	$E^{**}_{U(Ga-20\ wt\%\ In)}$/V	$E^{**}_{U(Ga-40\ wt\%\ In)}$/V	$E^{**}_{U(Ga-70\ wt\%\ In)}$/V
723	−2.218	−2.271	−2.328
751	−2.215	−2.265	−2.311
779	−2.179	−2.254	−2.307
872	−2.161	−2.223	−2.284
938	−2.126	−2.205	−2.241
1001	−2.098	−2.171	−2.226
1067	−2.061	−2.136	−2.209

$$\log\ \gamma_{\alpha-Pr(Ga-20wt\%\ In)} = 3.81 - \frac{12759}{T} \pm 0.11 \qquad [14]$$

$$\log\ \gamma_{\alpha-Pr(Ga-40wt\%\ In)} = 3.93 - \frac{12190}{T} \pm 0.12 \qquad [15]$$

$$\log\ \gamma_{\alpha-Pr(Ga-70wt\%\ In)} = 3.74 - \frac{11300}{T} \pm 0.14 \qquad [16]$$

Newton interpolation polynomial expression was obtained to develop three-dimensional graph on the basis of the functional dependence of the activity coefficients, temperature and the atomic radius of the bimetallic alloys. The universal mathematical Maple 17 software was used for this purpose. The three-dimensional graph log γ−1/r-1000/T is presented in Fig. 6.

Low values of the activity coefficients show the strong interaction between praseodymium and the liquid alloys, Table III. It was found that the activity coefficients decreased in the row from Ga to In. This phenomenon can be associated with changes in the composition and strength of intermetallic compounds in the range from gallium to indium. Rising temperature shifted the system towards more ideal behavior, in agreement with the literature.[45] The nonlinear dependence of the activity coefficients vs the composition of the bimetallic alloys implies the formation of mixed Me-Ga-In alloys or the presence of several (Me-Ga_n or Me-In_n) intermetallic compounds under equilibrium conditions.

An expression describing the relationship between the activity, solubility and activity coefficient are described by the expression (17)[29]:

$$\log\ a = \log\ x + \log\ \gamma \qquad [17]$$

In the above formula, α is the activity; x is the solubility and γ is the activity coefficient.

For calculation of the activity of solid Pr in saturated Pr-Ga-In alloys containing intermetallic compounds, the Eq. 18 was employed:

$$\log\ a = \frac{nF\Delta E}{2.303RT} \qquad [18]$$

where ΔE is the e.m.f. between the equilibrium potential of the couple ($E_{Pr^{3+}/Pr}$) and the equilibrium potentials of saturated alloy ($E_{Pr(Ga-In)}$), corresponds to a two-phase region (liquid + intermetallic compound), V.

The obtained results can be approximated by the Eqs. 19–21 in the studied temperature range:

$$\log\ a_{Pr(Ga-20wt\%\ In)} = 4.68 - \frac{15082}{T}0.15 \qquad [19]$$

$$\log\ a_{Pr(Ga-40wt\%\ In)} = 4.67 - \frac{14387}{T}0.15 \qquad [20]$$

$$\log\ a_{Pr(Ga-70wt\%\ In)} = 4.43 - \frac{13495}{T}0.18 \qquad [21]$$

The solubility of praseodymium in liquid gallium-indium alloys was calculated according to the expression (17). The results are presented in Table IV and by expressions (22–24):

$$\log\ x_{Pr(Ga-20\ wt\%\ In)} = 0.87 - \frac{2323}{T}\ 0.04 \qquad [22]$$

$$\log\ x_{Pr(Ga-40wt\%\ In)} = 0.74 - \frac{2197}{T}0.06 \qquad [23]$$

Table III. Activity coefficients of α-Pr in liquid bimetallic Ga-In alloys at different temperatures.

T/K	log γ_{Pr-Ga} Pr-Ga,[29]	log $\gamma_{Pr(Ga-In)}$ Pr-Ga-20 wt% In	log $\gamma_{Pr(Ga-In)}$ Pr-Ga-40 wt% In	log $\gamma_{Pr(Ga-In)}$ Pr-Ga-70 wt% In	log γ_{Pr-In} Pr-In,[29]
723	−14.46	−13.88	−13.03	−12.04	−10.50
751	−13.79	−13.19	−12.40	−11.33	−9.98
779	−13.18	−12.69	−11.84	−10.95	−9.50
872	−11.42	−10.88	−10.09	−9.34	−8.13
938	−10.38	−9.96	−9.17	−8.41	−7.32
1001	−9.52	−9.07	−8.35	−7.61	−6.65
1067	−8.72	−8.85	−7.59	−6.93	−6.03

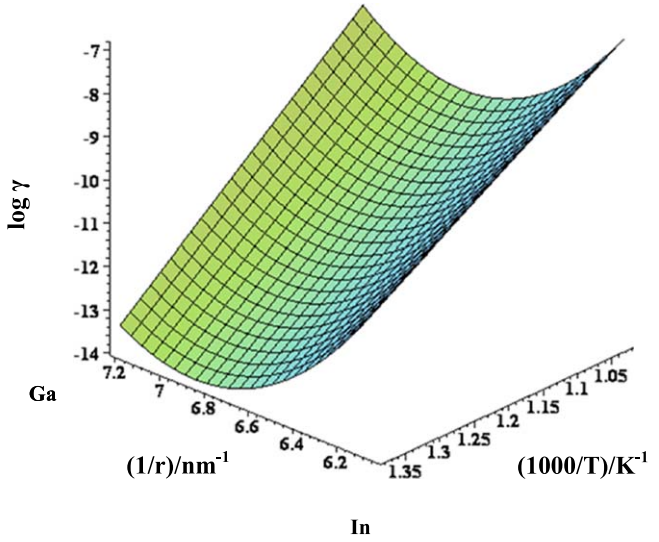

Figure 6. Three-dimensional relationship of activity coefficient (γ)—atomic radius (r)—temperature (T) for praseodymium in fused Pr(Ga-In)/LiCl-KCl-CsCl system. The effective radius of the atoms of the bimetallic alloy was calculated using the equation $r_e = (nr_{Ga} + mr_{In})$; where n and m is mole fraction of the components of the alloy; r is the atomic radius, nm.

$$\log\ x_{\mathrm{Pr}(Ga-70wt\%\ In)} = 0.69 - \frac{2195}{\mathrm{T}}0.07 \qquad [24]$$

The three-dimensional graph log x–1/r–1000/T is presented in Fig. 7. Data analysis shows that the composition of the bimetallic alloy shows a little effect on the solubility of praseodymium. An increasing of the temperature leads to a natural growth of the solubility of Pr in Ga-In alloys, Table IV.

The partial excess Gibbs free energy change of Pr in liquid Ga–In alloys was calculated according to Eq. 17 and previously obtained expressions (13–15):

$$\Delta G^{\mathrm{ex.}}_{\mathrm{Pr(Ga-In)}} = \Delta H_{\mathrm{Pr(Ga-In)}} - T\Delta S^{\mathrm{ex.}}_{\mathrm{Pr(Ga-In)}} \qquad [25]$$

$$\Delta G^{\mathrm{ex.}}_{\mathrm{Pr(Ga-In)}} = 2.303\mathrm{RT}\ \log\ \gamma_{\mathrm{Pr(Ga-In)}} \qquad [26]$$

$$\Delta G^{\mathrm{ex}}_{\mathrm{Pr(Ga-20wt\%\ In)}} = -243.8 + 0.072 \cdot T \pm 3.6 \quad \mathrm{kJ\ mol^{-1}} \qquad [27]$$

$$\Delta G^{\mathrm{ex}}_{\mathrm{Pr(Ga-40wt\%\ In)}} = -232.9 + 0.075 \cdot \mathrm{T} \pm 3.1 \quad \mathrm{kJ\ mol^{-1}} \qquad [28]$$

$$\Delta G^{\mathrm{ex}}_{\mathrm{Pr(Ga-70wt\%\ In)}} = -215.9 + 0.071 \cdot \mathrm{T} \pm 3.9 \quad \mathrm{kJ\ mol^{-1}} \qquad [29]$$

where $\Delta G^{\mathrm{ex.}}$ is the partial excess Gibbs free energy change, kJ mol^{-1}; ΔH is partial enthalpy change of mixing, kJ mol^{-1}; $\Delta S^{\mathrm{ex.}}$ is partial excess entropy change, J/mol·K.

The obtained results show the shift of partial enthalpy change of mixing towards more positive values with increasing of the concentration of indium in binary alloys.

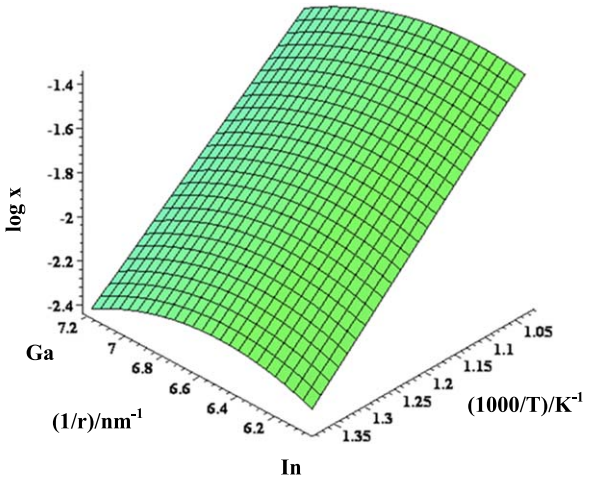

Figure 7. Three-dimensional relationship of solubility (x)—atomic radius (r)—temperature (T) for praseodymium in fused Pr(Ga-In)/LiCl-KCl-CsCl system. The effective radius of the atoms of the bimetallic alloy was calculated using the equation $r_e = (nr_{Ga} + mr_{In})$; where n and m is mole fraction of the components of the alloy; r is the atomic radius, nm.

The reaction scheme of alloy formation can be written as follows:

$$[\mathrm{MeCl_6}]^{n-} + \mathrm{ne} + \mathrm{n(xGa - yIn)} = \mathrm{Me(xGa - yIn)_n} + 6\mathrm{Cl^-} \qquad [30]$$

In the study of the separation of lanthanides and actinides, the effectiveness of using electrochemical separation methods is usually described by the value of the distribution or separation factor. The value of the separation factor is described by Eq. 30:

$$\log\ \theta = \frac{\mathrm{nF}}{2.303\mathrm{RT}}(\mathrm{E^{**}_{U(Ga-In)}} - \mathrm{E^{**}_{Pr(Ga-In)}}) \qquad [31]$$

where $\mathrm{E^{**}_{U(Ga-In)}}$ is the apparent standard potential of U–Ga–In alloy, V; $E^{**}_{\mathrm{Pr(Ga-In)}}$ is the apparent standard potential of Pr–Ga–In alloy, V; n, F, R, T are the standard values.

The calculated values of separation factor Pr/U vs the temperatures at various concentrations of indium in Ga-In alloys are presented in Fig. 8 and Table V.

$$\log\ \theta_{\mathrm{(Ga-20wt\%\ In)}} = -3.33 + \frac{6271}{\mathrm{T}} \pm 0.02 \qquad [32]$$

$$\log\ \theta_{\mathrm{(Ga-40wt\%\ In)}} = 3.35 - \frac{6022}{\mathrm{T}} \pm 0.02 \qquad [33]$$

$$\log\ \theta_{\mathrm{(Ga-70wt\%\ In)}} = 3.94 - \frac{6362}{\mathrm{T}} \pm 0.02 \qquad [34]$$

The separation factor of praseodymium-uranium couple in molten salt eutectic, calculated according to the above formula (31), indicates that uranium was concentrated in the alloy phase, while praseodymium—in molten salt phase. The results of

Table IV. Solubility of praseodymium in liquid bimetallic Ga-In alloys at different temperatures.

T/K	log x_{Pr-Ga} Pr-Ga,[29]	log $x_{\mathrm{Pr}(Ga-In)}$ Pr-Ga-20 wt% In	log $x_{\mathrm{Pr}(Ga-In)}$ Pr-Ga-40 wt% In	log $x_{\mathrm{Pr}(Ga-In)}$ Pr-Ga-70 wt% In	log x_{Pr-In} Pr-In,[29]
723	−2.43	−2.34	−2.30	−2.34	−2.35
751	−2.31	−2.22	−2.18	−2.23	−2.20
779	−2.20	−2.11	−2.08	−2.13	−2.07
872	−1.89	−1.79	−1.78	−1.82	−1.70
938	−1.70	−1.61	−1.60	−1.65	−1.48
1001	−1.55	−1.45	−1.46	−1.47	−1.30
1067	−1.41	−1.31	−1.32	−1.32	−1.13

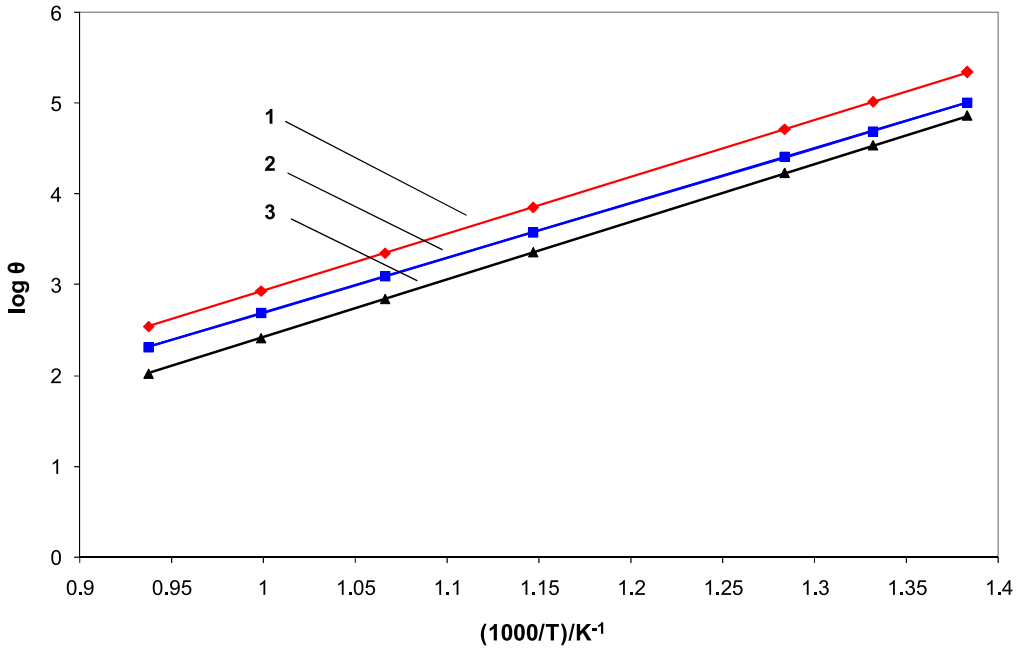

Figure 8. The dependence of the separation factor of uranium from praseodymium on liquid Ga-In alloy vs the temperature and concentration indium in alloy. 1—Pr-Ga-20 wt% In; 2—Pr-Ga-40 wt% In; 3—Pr-Ga-70 wt% In.

Table V. The separation factor of the couple U/Pr in fused Me(Ga-In)/LiCl-KCl-CsCl system at different temperatures.

	$\log \theta_{U/Pr}$			$\theta_{U/Pr}$		
T/K	Ga-20 wt% In	Ga-40 wt% In	Ga-70 wt% In	Ga-20 wt% In	Ga-40 wt% In	Ga-70 wt% In
723	5.39	5.11	4.86	$2.45 \cdot 10^5$	$1.29 \cdot 10^5$	$7.24 \cdot 10^4$
751	5.01	4.66	4.53	$1.02 \cdot 10^5$	$4.57 \cdot 10^4$	$3.39 \cdot 10^4$
779	4.71	4.45	4.23	$5.13 \cdot 10^4$	$1.71 \cdot 10^4$	$1.70 \cdot 10^4$
872	3.85	3.53	3.35	$7.08 \cdot 10^3$	$3.39 \cdot 10^3$	$2.24 \cdot 10^3$
938	3.35	2.95	2.84	$2.23 \cdot 10^3$	$8.91 \cdot 10^2$	$6.92 \cdot 10^2$
1001	2.93	2.66	2.41	$8.51 \cdot 10^2$	$4.57 \cdot 10^2$	$2.56 \cdot 10^2$
1067	2.54	2.38	2.02	$3.47 \cdot 10^2$	$2.40 \cdot 10^2$	$1.05 \cdot 10^2$

Table VI. The comparation of the separation factor of the couple U/Ln on liquid Ga—20 wt% In electrode at 723 K.

System	$\log \theta_{U/Ln}$	$\theta_{U/Ln}$	References
U/La couple	5.46	$2.88 \cdot 10^5$	47
U/Pr couple	5.39	$2.45 \cdot 10^5$	[this work]
U/Nd couple	5.08	$1.19 \cdot 10^5$	47

calculations show that high values of SF can be achieved only at low temperatures. Separation factor values decrease with the increasing temperature, due to the entropy factor. Within the range of parameters explored in this study it has been shown that the main parameters that have affected on the separation factor are the temperature and the composition of the liquid metal alloy. The obtained results are compared with the literature data and summarized in Table VI. It can be shown that for a subgroup of cerium lanthanides, the decrease of the separation factor in the range from La to Nd was registered, which is conformed with the theory of lanthanide compression in the row of lanthanides.[46]

Conclusions

The equilibrium potentials of Pr^{3+}/Pr couple, triple Pr-Ga-In and U-Ga-In alloys vs Cl^-/Cl_2 reference electrode at the temperature range 723-1073 K in fused LiCl-KCl-CsCl eutectic were carried out by open-circuit potentiometry. The apparent standard potentials of Pr^{3+}/Pr couple and triple alloys were determined. The principle thermodynamic properties, solubility and the activity coefficients of praseodymium in gallium-indium alloys, containing 20, 40 and 70 wt% indium were determined. It was established a strong interaction between atoms of Pr and liquid alloys. The separation factor of U/Pr couple vs the composition of gallium-indium alloys and the temperature were calculated.

ORCID

Alena Novoselova https://orcid.org/0000-0002-2338-0646
Valeri Smolenski https://orcid.org/0000-0002-8303-9626

References

1. T. Inoue and L. Koch, *Nucl. Eng. hnol.*, **40**, 183 (2008).
2. J. Zhang, *J. Nucl. Mater.*, **447**, 271 (2014).
3. J. J. Laidler, J. E. Battles, W. E. Miller, J. P. Ackerman, and E. L. Carls, *Prog. Nucl. Chem. Energy*, **31**, 131 (1997).
4. Y. Sakamura, T. Inoue, O. Shirai, T. Iwai, Y. Arai, and Y. Suzuki, *Proceedings of the International Conference on Future Nuclear Systems, GLOBAL'99, 29* August-2 September, Wyoming (1999).
5. K. Kinoshita, M. Kurata, and T. Inoue, *J. Nucl. Sci. Technol.*, **37**, 75 (2000).
6. H. P. Nawada and K. Fukuda, *J. Phys. Chem. Solids*, **66**, 647 (2005).
7. M. Kurata, Y. Sakamura, and T. Matsui, *J. Alloys Compd.*, **234**, 83 (1996).
8. Y. Castrillejo, M. R. Bermejo, P. D. Arocas, A. M. Martínez, and E. Barrado, *J. Electroanal. Chem.*, **579**, 343 (2005).

9. J. Zhang, E. A. Lahti, and W. Zhou, *J. Radioanal. Nucl. Chem.*, **303**, 1637 (2015).
10. M. Iizuka, T. Koyama, N. Kondo, R. Fujita, and H. Tanaka, *J. Nucl. Mater.*, **247**, 183 (1997).
11. Y. Sakamura, T. Hijikata, K. Kinoshita, T. Inoue, T. Storvick, C. Krueger, L. Grantham, S. Fusselman, D. Grimmett, and J. Roy, *J. Nucl. Sci. Technol.*, **35** (1998).
12. K. Uozumi, K. Kinoshita, T. Inoue, S. Fusselman, D. Grimmett, J. Roy, T. Storvick, C. Krueger, and C. Nabelek, *J. Nucl. Sci. Technol.*, **38**, 36 (2001).
13. T. Koyama, M. Iizuka, Y. Shoji, R. Fujita, H. Tanaka, T. Kobayashi, and M. Tokiwai, *J. Nucl. Sci. Technol.*, **34**, 384 (1997).
14. T. Murakami, Y. Sakamura, N. Akiyama, S. Kitawaki, A. Nakayoshi, and T. Koyama, *Procedia Chem.*, **7**, 798 (2012).
15. T. L. Reichmann and H. Ipser, *Metallurgical & Materials Transactions A*, **45**, 1171 (2014).
16. T. Koyama, M. Iizuka, N. Kondo, R. Fujita, and H. Tanaka, *J. Nucl. Mater.*, **247**, 227 (1997).
17. Y. Sakamura, O. Shirai, T. Iwai, and Y. Suzuki, *J. Electrochem. Soc.*, **147**, 642 (2000).
18. J. Zhang, E. A. Lahti, and E. Wu, *Prog. Nucl. Energ.*, **81**, 67 (2015).
19. T. Q. Yin, K. Liu, Y. L. Liu, Y. D. Yan, G. L. Wang, Z. F. Chai, and W. Q. Shi, *J. Electrochem. Soc.*, **165**, D722 (2018).
20. T. Q. Yin, K. Liu, Y. L. Liu, Y. D. Yan, G. L. Wang, Z. F. Chai, and W. Q. Shi, *J. Electrochem. Soc.*, **165**, D452 (2018).
21. L. Liu, L. Y. Yuan, L. Kui, G. A. Ye, M. L. Zhang, H. He, H. B. Tang, R. S. Lin, Z. F. Chai, and W. Q. Shi, *Electrochim. Acta*, **120**, 369 (2014).
22. Y. L. Liu, G. A. Ye, K. Liu, L. Y. Yuan, Z. F. Chai, and W. Q. Shi, *Electrochim. Acta*, **168**, 206 (2015).
23. L. X. Luo, Y. L. Liu, N. Liu, L. Wang, L. Y. Yuan, Z. F. Chai, and W. Q. Shi, *Electrochim. Acta*, **191**, 1026 (2016).
24. Y. L. Liu, Y. D. Yan, W. Han, M. L. Zhang, L. Y. Yuan, K. Liu, G. A. Ye, H. He, Z. F. Chai, and W. Q. Shi, *RSC Adv.*, **3**, 23539 (2013).
25. G. De Córdoba, A. Laplace, O. Conocar, J. Lacquement, and C. Caravaca, *Electrochim. Acta*, **54**, 280 (2008).
26. V. Smolenski and A. Novoselova, *Electrochim. Acta*, **63**, 179 (2012).
27. K. Liu, Y. L. Liu, Z. F. Chai, and W. Q. Shi, *J. Electrochem. Soc.*, **164**, D169 (2017).
28. J. Finne, G. Picard, S. Sanchez, E. Walle, O. Conocar, J. Lacquement, J. M. Boursier, and D. Noel, *J. Nucl. Mater.*, **344**, 165 (2005).
29. V. A. Lebedev, *Selectivity of Liquid Metal Electrodes in Molten Halide* (Metallurgiya, Chelyabinsk) (1993), (in Russian).
30. V. Smolenski, A. Novoselova, A. Osipenko, and A. Maershin, *Electrochim. Acta*, **145**, 81 (2014).
31. V. Smolenski, A. Novoselova, and V. A. Volkovich, *J. Nucl. Mater.*, **495**, 285 (2017).
32. V. Smolenski, A. Novoselova, A. Osipenko, M. Kormilitsyn, and Y. Luk'yanova, *Electrochim. Acta*, **133**, 354 (2014).
33. V. Smolenski, A. Novoselova, V. Volkovich, Y. Luk'yanova, A. Osipenko, A. Bychkov, and T. R. Griffiths, *J. Radioanal. Nucl. Chem.*, **311** (2017).
34. V. Smolenski, A. Novoselova, A. Bychkov, V. Volkovich, Y. Luk'yanova, and A. Osipenko, *Uranium—Safety, Resources, Separation and Thermodynamic Calculation* (IntechOpen, Rijeka) p. 109 (2018).
35. A. Novoselova and V. Smolenski, *J. Nucl. Mater.*, **509**, 313 (2018).
36. A. Novoselova, V. Smolenski, V. Volkovich, and Y. Luk'yanova, *J. Chem. Thermodynamics*, **130**, 228 (2019).
37. S. A. Kuznetsov, H. Hayashi, K. Minato, and M. Gaune-Escard, *Electrochim. Acta*, **51**, 2463 (2006).
38. K. Serrano and P. Taxil, *J. Appl. Electrochem.*, **29**, 497 (1999).
39. R. B. Prabhakara, S. Vandarkuzhali, T. Subramanian, and P. Venkatesh, *Electrochim. Acta*, **49**, 2471 (2004).
40. S. A. Kuznetsov, H. Hayashi, K. Minato, and M. Gaune-Escard, *J. Electrochem. Soc.*, **152**, C203 (2005).
41. D. Rappleye, K. Teaford, and M. F. Simpson, *Electrochim. Acta*, **219**, 721 (2016).
42. F. Gao, C. Wang, L. Liu, J. Guo, S. Chang, L. Chan, and Y. Ouyang, *J. Radioanalyt. Nucl. Chem.*, **280**, 207 (2009).
43. K. Liu, H. B. Tang, J. W. Pang, Y. L. Liu, Y. X. Feng, Z. F. Chai, and W. Q. Shi, *J. Electrochem. Soc.*, **163**, D554 (2016).
44. B. G. Korshunov, V. V. Safonov, and D. B. Drobot, *Phase Equilibria in Halide Systems* (Metallurgiya, Moscow) (1979), (in Russian).
45. G. Kaptay, *Metallurgical and Materials Transactions A*, **43**, 531 (2012).
46. V. Goldschmidt, *Geochemische Verteilungsgesetze Der Elemente, Skrifter Norske Videnskaps* (Akad, Oslo) (1926).
47. V. Smolenski, A. Novoselova, V. Volkovich, A. Bychkov, Y. Luk'yanova, and A. Osipenko, *Proceedings of the International Conference on Fast Reactors and Related Fuel Cycles: Next Generation Nuclear Systems for Sustainable Development*, IAEA, Vienna, 245 (2018).